Rectifying characteristics and transport behavior of $SrTiO_{3-\delta}(110)/p$-Si (100) heterojunctions

Z. Luo
Department of Physics, The University of Hong Kong, Hong Kong, China

J. H. Hao
Department of Applied Physics, The Hong Kong Polytechnic University, Hong Kong, China

J. Gao[a)]
Department of Physics, The University of Hong Kong, Hong Kong, China

(Received 9 March 2007; accepted 10 July 2007; published online 7 August 2007)

Introducing oxygen vacancy causes the dielectric insulator $SrTiO_3$ to evolve to a *n*-type semiconductor. The authors have fabricated n-$SrTiO_{3-\delta}(110)/p$-Si (100) heterojunctions, showing clear rectifying characteristics at different temperatures from 100 to 292 K. A forward-to-reverse bias ratio of about 1200 was found at $V=\pm 2$ V for the *p-n* junction operated at $T=292$ K. The current-voltage characteristic follows $I \propto \exp(eV/\eta kT)$ for the *p-n* junction at relatively low forward-bias voltage, while the relation of $I \sim V^{1.9}$ describes the transport behavior of *p-n* junction at relatively high forward-bias voltage. The measured results have been discussed in Anderson model and space charge limited model. © *2007 American Institute of Physics*.
[DOI: 10.1063/1.2767999]

Strontium titanate is an incipient ferroelectric material with a relatively high dielectric constant. Thin films of strontium titanate were reported to grow on Si (001),[1,2] which is one of promising candidates to replace SiO_2 as a gate oxide for next generation complementary metal-oxide-semiconductor devices. On the other hand, strontium titanate can be changed from an insulator to a *n*-type semiconductor by introducing oxygen vacancy or impurity doping.[3,4] Thus, *p-n* heterojunctions can be formed by growing a layer of oxygen deficient $SrTiO_{3-\delta}$ (STO) on a *p*-type Si in a high vacuum environment. Earlier studies have demonstrated the clear rectifying characteristic and ultraviolet photovoltage in the heterojunctions of STO (100)/*p*-Si (100).[5,6] The substrate induced strain may have great influence on the properties of STO thin films. A significant in-plane anisotropy in dielectric constant and tuning, resulting from the structure distortion, has been observed in thin films of strontium titanate deposited on $DyScO_3$.[7] In addition, studies on the Nb-doped $SrTiO_3$ grown on different substrates suggested that substrate-induced strain results in highly resistive states.[8] The key role of lattice distortion has also been observed in magnetoresistance manganites.[9] In order to investigate this issue extensively, we have previously reported on the preparation of thin films of strontium titanate with (110) out-of-plane orientation grown directly on Si substrate.[10,11] In this letter, the electrical and transport properties of n-STO(110)/*p*-Si (100) heterojunction have been investigated in detail.

Epitaxial STO (110) films were grown on *p*-Si (100) by pulsed laser deposition technique using a KrF excimer laser ($\lambda=248$ nm) with a repetition rate of 5 Hz. During the deposition procedure, the substrate temperature was kept at about 780 °C and the oxygen partial pressure maintained at 1.4×10^{-3} mbar. The deposited films were then *in situ* annealed in high vacuum at about 840 °C for a few hours. The film thickness was about 850 nm. In order to study the current-voltage (*I-V*) characteristics across the STO/Si junction, Ag electrodes with a diameter of about 0.7 mm were fabricated by thermal evaporation.

Figure 1 displays a typical x-ray diffraction pattern of STO (110)/Si (100). Only diffraction peaks of STO (110) and (220) were observed in addition to the peaks from Si substrate. This suggests that the grown film has an (110) out-of-plane orientation. The peak of STO (110) face has a 2θ value of 32.44°. The lattice constant of $SrTiO_3$ and Si is $a_{STO}=0.3905$ nm and $a_{Si}=0.5430$ nm, respectively.[11] For $SrTiO_3$ (100)/Si (100), the lattice mismatch is $(|a_{STO}-a_{Si}|/a_{Si})\times100\%=28\%$. This value is very large for a good epitaxial growth. However, if STO lattice rotates 45° in plane with respect to Si lattice, the mismatch would be very small, $(|\sqrt{2}a_{STO}-a_{Si}|/a_{Si})\times100\%=1.7\%$. Our previous studies suggested that the in-plane alignments of STO (110) on Si (100) are STO[001]∥Si[001] and STO $[1\bar{1}0]$∥Si[010].[10,11] The lattice mismatches in STO $[1\bar{1}0]$ and STO [001] directions are 1.7 and 28%, respectively. The epitaxial STO ultrathin film is usually severely strained. The strain relaxes as

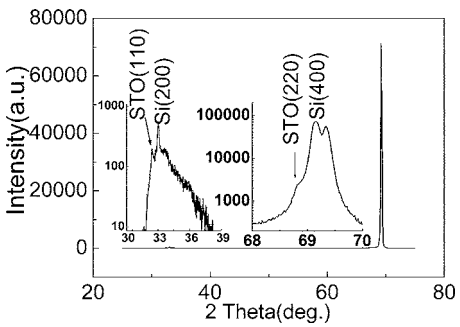

FIG. 1. Typical x-ray diffraction spectra of $SrTiO_{3-\delta}$/Si. Inset shows the diffraction peaks in semilog scale.

a)Author to whom correspondence should be addressed; electronic mail: jugao@hku.hk

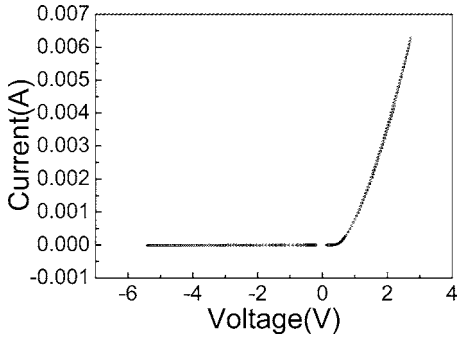

FIG. 2. Typical *I-V* curve of $SrTiO_{3-\delta}$ (110)/*p*-Si (100) heterojunction at 292 K.

thickness increases. In the case of our 850-nm-thick film, the strain is expected to relax well. It reflects that a lattice parameter of STO film is very close to that of corresponding bulk material.

I-V characteristics across the STO/*p*-Si junction were carefully studied. A typical *I-V* curve at $T=292$ K was shown in Fig. 2. Forward bias was defined as a positive pole of dc voltage applied on the *p*-Si. The *p-n* junction demonstrates striking rectification. Under forward bias, the current is very small (~ 1 μA at 0.23 V) at the beginning and starts to increase very quickly after the bias voltage exceeds a threshold value of about 0.5 V. However, it remains very small even under large reverse bias. A forward-to-reverse current ratio of about 1200 occurs at ±2 V. The observed phenomena can be explained by considering the band structure of the STO/*p*-Si heterojunction and the band structure of STO/*p*-Si heterojunction can be constructed by Anderson model (Fig. 3). Values of electron affinity [χ(Si)=4.05 eV (Ref. 12) and χ(STO)=3.9 eV (Ref. 13)] and band gap [E_g(Si)=1.12 eV (Ref. 12) and E_g(STO)=3.3 eV (Ref. 13)] were taken in the procedure of constructing the band structure. The band offset of conduction band at STO/*p*-Si interface is $\Delta E_c=\chi(\mathrm{STO})-\chi(\mathrm{Si})=-0.15$ eV and that of valance band is $\Delta E_v=[\chi(\mathrm{STO})-\chi(\mathrm{Si})]+[E_g(\mathrm{STO})-E_g(\mathrm{Si})]=2.03$ eV. This is consistent with the result reported by Chamgbers *et al.*[14] An energy barrier is formed at the interface of STO/Si. Under forward bias condition, the applied voltage reduces the energy barrier, and electrons in the conduction band of STO may inject into that of *p*-Si. In the Anderson model, the relationship between the current and the applied voltage across the junction can be expressed as[15]

$$I = A \exp\left[-\frac{q(V_d - \Delta E_c)}{kT}\right] \times \left[\exp\left(\frac{qV}{kT}\right) - 1\right], \tag{1}$$

where V is the voltage applied to the junction, k is the Boltzmann constant, T is the absolute temperature,

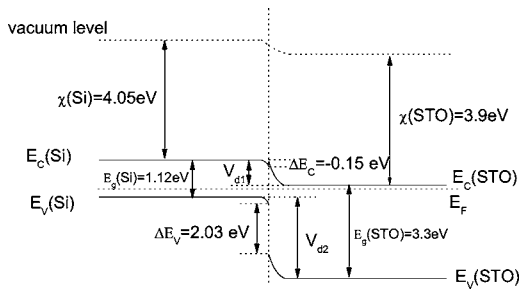

FIG. 3. Band structure of of $SrTiO_{3-\delta}$ (110)/*p*-Si (100) based on Anderson model.

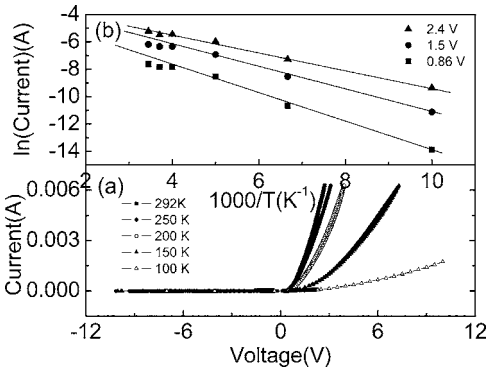

FIG. 4. *I-V* curve of $SrTiO_{3-\delta}$ (110)/*p*-Si (100) heterojunction at different temperatures (a) and ln(*I*)-(1000/*T*) under bias voltages of 2.4, 1.5, and 0.86 V (b).

$V_d=V_{d1}+V_{d2}$, and $A=aqXN_{D2}(D_{n1}/\tau_{n1})^{1/2}$, where a is the junction area, X is the transmission coefficient for the electrons across the interface, and D_{n1} and τ_{n1} are the diffusion constant and lift time for *p*-Si, respectively. When $qV \gg kT$,

$$I = A \exp\left\{\frac{q[V - (V_d - \Delta E_c)]}{kT}\right\}. \tag{2}$$

Equation (2) indicates that the junction current increases exponentially with $V-(V_d-\Delta E_c)$.

Forward bias *I-V* characteristics were investigated at various temperatures from 100 to 292 K. In Fig. 4(a), one can see that the temperature dependence of *I-V* characteristic in the presented STO(110)/*p*-Si (100) heterojunction is quite similar to that of STO(100)/*p*-Si (100) heterojunctions.[5,6] As temperature decreases, the threshold voltage is enhanced and current under the same bias voltage is reduced. Figure 4(b) shows that the ln I is proportional to $1/T$ in low bias voltage range. This is consistent with Eq. (2). However, at a high temperature, the experimental data deviated from expected values. This implies that other transport mechanism may dominate the transport properties of *p-n* junction under that condition.

In Anderson model, the effect of the interface state is neglected. Detailed process of the carrier transport at the interface is not taken into account. However, carrier emission, recombination, and tunneling at the interface may have great influence. Considering these factors, the current-voltage relation can be empirically expressed as $I \propto \exp(eV/\eta kT)$.[12] Figure 5 shows the ln(*I*)-*V* relationship under forward bias at 292 K. By fitting the ln(*I*)-*V* curve, we obtained $\eta=2.1$ and $\eta=42$ in low and high forward bias

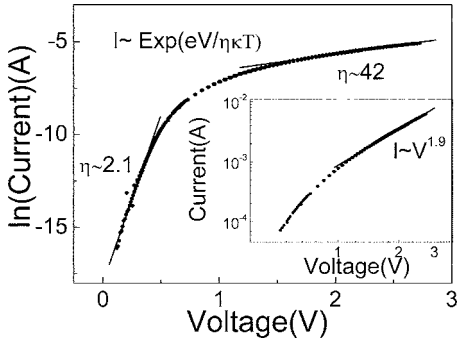

FIG. 5. ln(*I*)-*V* relation under forward bias at 292 K. Inset is the *I-V* curve in log-log scale.

voltage regions, respectively. In high forward bias region, the value of 42 is too large for fitting the relationship $I \propto \exp(eV/\eta kT)$. Plotting the *I-V* curve in log-log scale (inset of Fig. 5), we found that it follows $I \sim V^{1.9}$ in the range of high voltage bias. Similar phenomenon was observed in other semiconductor structures.[16] It was attributed to a model of space charge limited current conduction. Under low forward bias, the dielectric relaxation time t_D is much smaller than the carrier diffusion-length time t_0. Holes and electrons swept into space charge region (SCR) are recombined in SCR, maintaining charge neutrality. When the bias voltage is very high, holes will transverse SCR and recombine with major electrons in STO. If all electrons in the doping level of STO are depleted, the junction conductance can be analogous to conductance in solid insulator and the current will be space charge limited. The current-voltage relation will follow $J=(9/8)\varepsilon\mu V^2/d^3$. The character and the magnitude of space charge limit depend on the density, location, and capture cross sections of the trapping states.[17] Strain effect changes Ti–O–Ti bond length and angle, leading to a change in the electronic band structure of STO. Although strain could be relaxed in thick films, however, the strain in the bottom layer near the interface may still remain. Oxygen pressure and substrate temperature have great influence on the carrier density and microstructure of STO films too. Further investigation is necessary to understand the role of these factors in determining the transport properties of STO/Si heterojunction.

In conclusion, the *I-V* characteristics of *n*-STO(110)/*p*-Si(100) heterojunction were studied systematically. Under low forward bias, the transport mechanism was determined by the energy band structures of STO and *p*-Si. While under high forward bias, the conduction becomes space charge limited and follows $I \sim V^{1.9}$. The transport properties of STO(110)/*p*-Si (100) heterojunctions are similar to those of STO(100)/*p*-Si (100) heterojunctions. To understand the underlying physics of STO/Si heterojunctions, various factors such as lattice strain and oxygen deficiency should also be taken into account.

This work has been supported by the Research Grant Council of Hong Kong (Project Nos. HKU 7025/06P and PolyU 7025/05P) and the CRCG of the University of Hong Kong.

[1]X. M. Hu, H. Li, Y. Liang, Y. Wei, Z. Yu, D. Marshall, J. Edwards, R. Droopad, X. Zhang, A. A. Demkov, K. Moore, and J. Kulik, Appl. Phys. Lett. **82**, 203 (2003).
[2]R. A. McKee, F. J. Walker, and M. F. Chisholm, Phys. Rev. Lett. **81**, 3014 (1998).
[3]N. Shanthi and D. D. Sarma, Phys. Rev. B **57**, 2153 (1998).
[4]T. Tomio, H. Miki, H. Tabata, T. Kawai, and S. Kawai, J. Appl. Phys. **76**, 5886 (1994).
[5]H. Z. Guo, Y. H. Huang, K. J. Jin, Q. L. Zhou, H. B. Lu, L. F. Liu, Y. L. Zhou, B. L. Cheng, and Z. H. Chen, Appl. Phys. Lett. **86**, 123502 (2005).
[6]K. Zhao, Y. H. Huang, Q. L. Zhou, K. J. Jin, H. B. Lu, M. He, B. L. Cheng, Y. L. Zhou, Z. H. Chen, and G. Z. Yang, Appl. Phys. Lett. **86**, 221917 (2005).
[7]W. T. Chang, S. W. Kirchoefer, J. A. Bellotti, S. B. Qadri, J. M. Pond, J. H. Haeni, and D. G. Schlom, J. Appl. Phys. **98**, 024107 (2005).
[8]W. Ramadan, S. B. Ogale, S. Dhar, S. X. Zhang, D. C. Kundaliya, I. Satoh, and T. Venkatesan, Appl. Phys. Lett. **88**, 142903 (2006).
[9]A. Biswas, M. Rajeswari, R. C. Srivastava, Y. H. Li, T. Venkatesan, R. L. Greene, and A. J. Millis, Phys. Rev. B **61**, 9665 (2000).
[10]J. H. Hao, J. Gao, and H. K. Wong, Appl. Phys. A: Mater. Sci. Process. **81**, 1233 (2005).
[11]J. H. Hao, J. Gao, Z. Wang, and D. P. Yu, Appl. Phys. Lett. **87**, 131908 (2005).
[12]S. M. Sze, and Kwok K. Ng, *Physics of Semiconductor Devices*, 3rd ed. (Wiley, New York, 2007), p. 790.
[13]J. Robertson and C. W. Chen, Appl. Phys. Lett. **74**, 1168 (1999).
[14]S. A. Chambers, Y. Liang, Z. Yu, R. Droopad, J. Ramdani, and K. Eisenbeiser, Appl. Phys. Lett. **77**, 1662 (2000).
[15]B. L. Sharma and R. K. Purohit, *Semiconductor Heterojunctions*, 1st ed. (Pergamon, Oxford, 1974), 25.
[16]X. D. Chen, C. C. Ling, S. Fung, C. D. Beling, Y. F. Mei, R. K. Y. Fu, G. G. Siu, and P. K. Chu, Appl. Phys. Lett. **88**, 132104 (2006).
[17]M. A. Lampert, *Current Injection in Solids* (Academic, New York, 1970).